arXiv:hep-lat/0307023 v1 14 Jul 2003

FERMILAB-Pub-03/197-T

Chiral Lagrangian Parameters for Scalar and Pseudoscalar Mesons

W. Bardeen[1], E. Eichten[1], and H. Thacker[2]

[1]Fermilab, P.O. Box 500, Batavia, IL 60510

[2]Dept.of Physics, University of Virginia, Charlottesville, VA 22901

Abstract

The results of a high-statistics study of scalar and pseudoscalar meson propagators in quenched lattice QCD are presented. For two values of lattice spacing, $\beta = 5.7$ ($a \approx .18$ fm) and 5.9 ($a \approx .12$ fm), we probe the light quark mass region using clover improved Wilson fermions with the MQA pole-shifting ansatz to treat the exceptional configuration problem. The quenched chiral loop parameters m_0 and α_Φ are determined from a study of the pseudoscalar hairpin correlator. From a global fit to the meson correlators, estimates are obtained for the relevant chiral Lagrangian parameters, including the Leutwyler parameters L_5 and L_8. Using the parameters obtained from the singlet and nonsinglet pseudoscalar correlators, the quenched chiral loop effect in the nonsinglet scalar meson correlator is studied. By removing this QCL effect from the lattice correlator, we obtain the mass and decay constant of the ground state scalar, isovector meson a_0.

1 Introduction

Improved methods for studying the regime of small quark mass in lattice QCD provide the realistic prospect of quantitatively determining the parameters of the low energy chiral Lagrangian of QCD from first principles. Although a definitive comparison with experiment requires the analysis of full and/or partially quenched simulations, detailed studies of chiral behavior in the quenched approximation are of interest for several reasons. First, the characteristic quenched chiral loop effects which arise from the anomalous double-pole structure of the quenched, flavor-singlet pseudoscalar propagator will also occur in partially quenched calculations (at a level determined by the mismatch between valence and sea quark masses)[1]. The observation of these anomalous effects in the quenched theory should provide a useful baseline for future chiral analysis of full QCD. Second, although it is not a unitary theory, the quenched approximation can be analyzed in an effective Lagrangian framework[2, 3], yielding a well-defined set of low-energy constants in quenched chiral perturbation theory. (In practice, this requires the assumption that the $U_A(1)$ breaking from the anomaly can also be treated perturbatively). Comparison of these constants with those of full QCD can provide valuable insight into the role of closed quark loops in hadron phenomenology. In addition, the study of chiral behavior in the quenched approximation provides useful information about the interplay between topological charge and chiral symmetry breaking in QCD. For example, the Witten-Veneziano formula relates the gluonic component of the η' mass in full QCD to the topological susceptibility of the quenched theory.

In two previous papers [4, 5] we reported results of a study of the chiral behavior of scalar and pseudoscalar meson propagators in quenched QCD at $\beta = 5.7$ using clover improved Wilson fermions. In this paper we present results from a new data set at $\beta = 5.9$ [6], compare them with the $\beta = 5.7$ results, and summarize the main conclusions of

this study. We also compare our results to those of other recent studies.[7] An important ingredient in our analysis is the use of the MQA pole-shifting procedure [9] to resolve the exceptional configuration problem. Our experience with this technique has led us to conclude that it provides a practical and quantitatively acceptable resolution of the problem, which eliminates the spurious statistical fluctuations of exceptional configurations without systematically biasing the final results. This conclusion is based on the consistency between the light-quark results and those of heavier quarks where the pole-shifting has a negligible effect on the propagators. It is also supported by the overall agreement we observe between our results (in and out of the pole region) and theoretical expectations based on quenched chiral perturbation theory. (See Section 6)

Since the introduction of the MQA procedure, other methods for avoiding the exceptional configuration problem have been explored. These include twisted-mass QCD [10] and the use of exactly chiral (overlap [11] or domain-wall [12]) fermions. All these approaches have in common the fact that Wilson-Dirac eigenvalues at positive real quark mass are eliminated, thus resolving the problem. It should be noted that exactly real eigenmodes of the Wilson-Dirac operator, which are the cause of the exceptional configuration problem, make a negligible contribution to physical quantities in the infinite volume limit (vanishing like $1/\sqrt{V}$). Thus any prescription which effectively removes these poles from the physical region should provide a satisfactory resolution of the problem for sufficiently large volume. The MQA pole shifting is a minimal prescription for accomplishing this. A more stringent test of the procedure is the study of chiral behavior for very light quarks in a *finite* volume which is large compared to the QCD scale but comparable to the chiral scale. In this regime, finite volume effects are large but calculable in $Q\chi PT$, simply by replacing loop integrals by finite-volume momentum sums. As discussed in [5], the scalar, isovector (valence) meson propagator exhibits a prominent quenched chiral loop effect arising from the η'-π interme-

diate state. For the lightest quark masses we study, the finite volume effects expected from $Q\chi PT$ are quite large. Thus, the detailed agreement (as a function of both time and pion mass) between the measured scalar propagator and the *finite-volume* one-loop calculation provides a convincing demonstration that the MQA procedure is an effective method for exploring the light quark regime with Wilson fermions.

2 Quenched Chiral Perturbation Theory

To analyze the quenched theory in a chiral Lagrangian framework, one introduces wrong-statistics ghost quark fields to cancel closed loops, yielding a low-energy chiral Lagrangian with a graded $U(3|3) \times U(3|3)$ symmetry [2]. At the one-loop level, this is equivalent to the simpler and more direct approach to quenched χPT [3] which begins with an ordinary $U(3) \times U(3)$ chiral Lagrangian describing a nonet of Goldstone bosons. To leading order, this is

$$\mathcal{L}_2 = \frac{f^2}{4}\left[Tr(\partial_\mu U^\dagger \partial^\mu U) + Tr(\chi^\dagger U + U^\dagger \chi)\right] \tag{1}$$

where U is a $U(3) \times U(3)$ chiral field and χ is the pseudoscalar mass matrix. Our analysis also incorporates the following fourth-order terms in the chiral Lagrangian [14],

$$\mathcal{L}_4 = L_5 Tr(\partial_\mu U^\dagger \partial^\mu U(\chi^\dagger U + U^\dagger \chi)) + L_8 Tr(\chi^\dagger U \chi^\dagger U + U^\dagger \chi U^\dagger \chi) \tag{2}$$

The effect of the axial U(1) anomaly is introduced as an explicit symmetry breaking term consisting of a flavor-singlet pseudoscalar η' mass term and a field renormalization,

$$\mathcal{L}_{hp} = \frac{1}{2}(\alpha_\Phi \partial^\mu \eta' \partial_\mu \eta' - m_0^2 \eta'^2) \tag{3}$$

where

$$\eta' = \frac{f}{2}\left(iTr\ln(U^\dagger) - iTr\ln(U)\right) \tag{4}$$

Finally, we will also analyze the scalar, isovector meson propagator, which turns out to be well-described by a combination of a heavy a_0 meson and an η'-π loop diagram. Thus, we incorporate a scalar-isovector meson field, using the formalism of nonlinear chiral Lagrangians [4],

$$\mathcal{L}_{sc} = \frac{1}{4} tr\{D\sigma D\sigma\} - \frac{1}{4} m_s^2 tr\{\sigma\sigma\} + f_s tr\{\chi^\dagger \sqrt{U}\sigma\sqrt{U} + \chi\sqrt{U}^\dagger\sigma\sqrt{U}^\dagger\} \tag{5}$$

where D is a chirally covariant derivative. One of our motivations for studying the scalar correlator is the expectation of a prominent quenched chiral loop effect from the η'-π intermediate state, as discussed in Ref. [5]. The agreement between the lattice correlator and the one-loop calculation is very good, particularly for the $\beta = 5.9$ results, as discussed in Section 6.

To summarize, the low energy chiral Lagrangian used in our analysis is

$$\mathcal{L} = \mathcal{L}_2 + \mathcal{L}_4 + \mathcal{L}_{hp} + \mathcal{L}_{sc} \tag{6}$$

In the quenched approximation, we have the supplementary rule that multiple η' mass insertions on a given pseudoscalar line are excluded. More generally, any χPT diagram corresponding to a quark-line diagram with internal closed loops is discarded [3]. At the one-chiral-loop level, these rules are unambiguous, and equivalent to the more systematic procedure of introducing ghost fields [2].

3 Lattice Parameters

The calculations discussed in this paper were carried out on the Fermilab ACPMAPS and on the UVA Linux cluster GARCIA. The two Monte Carlo gauge ensembles analyzed consisted of 300 configurations at $\beta = 5.7$ on a $12^3 \times 24$ lattice, and 350 configurations at $\beta = 5.9$ on a $16^3 \times 32$ lattice (the Fermilab b and c ensembles). Quark propagators were calculated with

clover improved Wilson action. The clover coefficients used were $C_{sw} = 1.57$ for $\beta = 5.7$ and $C_{sw} = 1.50$ for $\beta = 5.9$. For $\beta = 5.7$, the quark propagators were calculated for $\kappa = .1410, .1415, .1420, .1423, .1425, .1427$, and .1428, with $\kappa_c = .14329$, while for $\beta = 5.9$, propagators were calculated with $\kappa = .1382, .1385, .1388, .1391, .1394$, and .1397, with $\kappa_c = .14013$. In physical units, this corresponds to a range of pion masses of 275 to 565 MeV for $\beta = 5.7$ and 330 to 665 MeV for $\beta = 5.9$. Here and elsewhere, we will quote results in physical units using the rho mass to set the scale.

An analysis of smeared and local rho propagators on our ensembles yields $m_\rho a = .690(8)$ and .469(3) for $\beta = 5.7$ and $\beta = 5.9$, respectively. An analysis of the axial-vector meson channel also yields a mass for the a_1 meson of 1.15(7) and 0.77(3) for $\beta = 5.7$ and $\beta = 5.9$ respectively. Using the rho mass to fix the scale gives $a^{-1} = 1.12$ GeV for $\beta = 5.7$ and 1.64 GeV for $\beta = 5.9$. The resulting physical mass for the a_1 (1290 MeV for $\beta = 5.7$ and 1260 MeV for $\beta = 5.9$) is close to the mass of the observed $a_1(1260)$ resonance.

To get some idea of the systematic error associated with choice of scale, we will sometimes quote equivalent results using the charmonium 1S-1P splitting scales of 1.18 GeV and 1.80 GeV for the two ensembles. The MQA pole-shifting procedure [9] was applied to all quark propagators. For $\beta = 5.7$, all poles below $\kappa = .1431$ were located and shifted, while for $\beta = 5.9$, all poles below $\kappa = .1400$ were shifted.

4 The Hairpin Insertion, η' Mass, and Topological Susceptibility

We begin by determining the parameters m_0 and α_Φ in the term $\mathcal{L}_{hp}$, Eq. (3). These parameters are extracted from the two-quark-loop ("disconnected") piece of the quenched

flavor singlet pseudoscalar correlator,

$$\Delta_h(x) = \langle Tr\gamma^5 G(x,x) Tr\gamma^5 G(0,0)\rangle \tag{7}$$

The lowest order $Q\chi PT$ approximation to (7) is the tree graph with a single hairpin insertion between two pion propagators. In momentum space, this is

$$\tilde{\Delta}_h(p) = f_P \frac{1}{p^2 + m_\pi^2} \left(m_0^2 + \alpha_\Phi p^2\right) \frac{1}{p^2 + m_\pi^2} f_P \tag{8}$$

where f_P is the pseudoscalar decay constant,

$$f_P = \langle 0|\bar{\psi}\gamma^5\psi|\pi\rangle \tag{9}$$

Fourier transforming over p_0 and setting $\vec{p} = 0$, we have

$$\Delta_h(\vec{p}=0,t) = \frac{f_P^2}{4m_\pi^3}\left[C_+ + C_- m_\pi t\right] e^{-m_\pi t} + (t \to T - t) \tag{10}$$

where

$$C_\pm \equiv m_0^2 \pm \alpha_\Phi m_\pi^2 \tag{11}$$

In our previous analysis of the $\beta = 5.7$ ensemble, the hairpin correlator Δ_h was studied for both local and smeared sources and compared with the pion pole residues of the corresponding valence propagators. This analysis demonstrated a remarkable absence of excited state contamination in the hairpin correlator, even when the sources were only separated by one or two time slices. Moreover, the time-dependence of $\Delta_h(t)$ was well-described at all times $t \geq 2$ by the formula (10) with $\alpha_\Phi = 0$, i.e. by a pure momentum-independent mass insertion. For the present analysis, we have fit both the 5.7 and 5.9 ensembles to the full two-parameter formula (10) in order to obtain an accurate estimate of α_Φ. For the 5.7 ensemble, acceptable χ^2's were obtained by fitting a range of times from $t = 3$ to 12. Using the fully correlated error matrix, the covariant χ^2 for these fits ranged from 0.8 to 1.5 per degree of freedom. For the hairpin correlators at $\beta = 5.9$, we obtained very good fits to the

formula (10) over the entire time range from $t = 1$ to 16. Here the correlated χ^2's ranged from 0.3 to 0.5 per degree of freedom. An example of a hairpin fit for $\beta = 5.9$ and $\kappa = .1394$ is shown in Fig. 1. The solid line is the pure dipole fit with $\alpha_\Phi = 0$. In Tables 1 and 2 we give the $\beta = 5.7$ and 5.9 results for m_0 and α_Φ. Also shown in the last column are the values of m_0 obtained from the 1-parameter pure dipole fit with $\alpha_\Phi = 0$. Considering first the results for α_Φ, the values for the 5.7 ensemble are negative by about one to two standard deviations, while the values for $\beta = 5.9$ are slightly positive, also by about two standard deviations. The values for different κ's within each ensemble are highly correlated, so the deviation of α_Φ from zero in either data set has little statistical significance. Ignoring κ-dependence and averaging the values within each ensemble, we get

$$\alpha_\Phi = -0.15 \pm 0.10, \quad \beta = 5.7 \tag{12}$$

and

$$\alpha_\Phi = 0.05 \pm 0.03, \quad \beta = 5.9. \tag{13}$$

If we ignore any possible lattice spacing dependence and average the two data sets in quadrature, we get the final result

$$\alpha_\Phi = 0.03 \pm 0.03 \tag{14}$$

This can be regarded as a success of the large-N_c view of the anomaly where this renormalization is an order $1/N_c$ effect. In the subsequent analysis we will take $\alpha_\Phi = 0$.

Fitting the hairpin correlators to the pure dipole $\alpha_\Phi = 0$ form (last column of Tables 1 and 2) we obtain the chirally extrapolated values (in lattice units)

$$m_0 = .348(4), \quad \beta = 5.7 \tag{15}$$

and

$$m_0 = .232(4), \quad \beta = 5.9. \tag{16}$$

Table 1: Fit parameters m_0 and α_Φ for the $\beta = 5.7$ hairpin correlators. All masses are in lattice units.

κ	m_π	m_0	α_Φ	$m_0(\alpha_\Phi = 0)$
.1410	.505(2)	.269(26)	-.17(10)	.280(10)
.1415	.450(3)	.291(24)	-.18(10)	.294(10)
.1420	.386(3)	.310(21)	-.19(10)	.308(10)
.1423	.342(4)	.321(19)	-.19(10)	.316(10)
.1425	.307(4)	.326(19)	-.16(11)	.321(10)
.1427	.267(5)	.326(19)	-.10(12)	.322(11)
.1428	.245(6)	.323(19)	-.03(13)	.322(11)

Table 2: Fit parameters m_0 and α_Φ for the $\beta = 5.9$ hairpin correlators. All masses are in lattice units.

κ	m_π	m_0	α_Φ	$m_0(\alpha_\Phi = 0)$
.1382	.411(3)	.188(14)	.04(2)	.194(5)
.1385	.378(3)	.192(13)	.04(2)	.198(5)
.1388	.343(4)	.197(11)	.04(2)	.203(5)
.1391	.304(4)	.204(11)	.05(2)	.209(5)
.1394	.261(5)	.211(9)	.06(3)	.217(5)
.1397	.204(5)	.220(9)	.11(4)	.226(6)

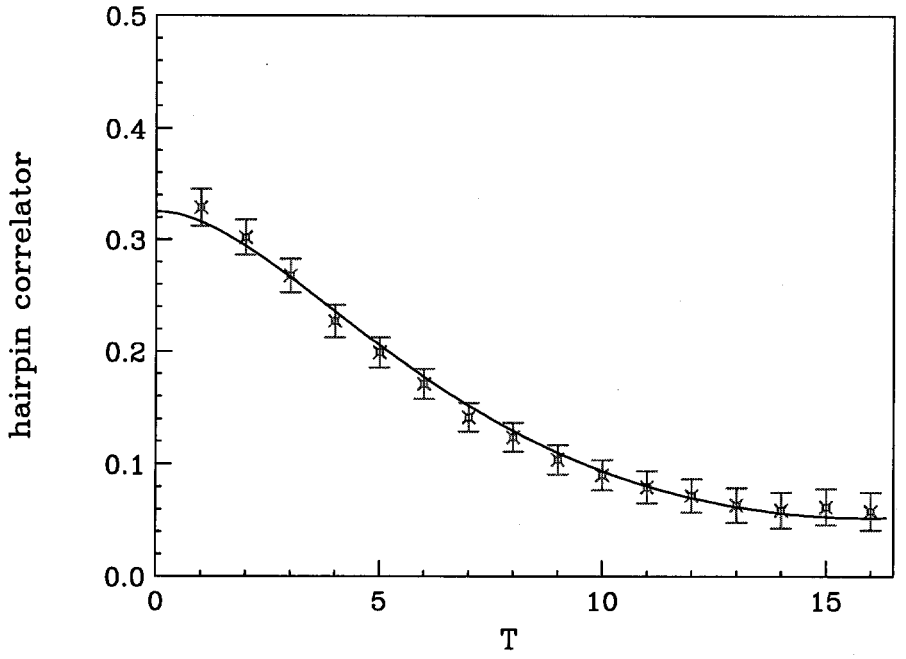

Figure 1: The quenched hairpin correlator for $\beta = 5.9$, $\kappa = .1394$. The solid line is a pure dipole fit with $\alpha_\Phi = 0$.

Using the rho mass scale and including a flavor factor of $\sqrt{3}$, this gives the gluonic component of the η' mass

$$m_{\eta'}^{glue} = 675(8) \text{ MeV}, \quad \beta = 5.7 \tag{17}$$

$$= 659(12) \text{ MeV}, \quad \beta = 5.9 \tag{18}$$

If we instead use the charmonium scale we get

$$m_{\eta'}^{glue} = 712(9) \text{ MeV}, \quad \beta = 5.7 \tag{19}$$

$$= 723(13) \text{ MeV}, \quad \beta = 5.9 \tag{20}$$

We conclude that the η' mass scales reasonably well between $\beta = 5.7$ and 5.9, well within the systematic uncertainty associated with different ways of determining the lattice spacing. The values we obtain for the η' mass insertion are somewhat low compared to the estimate of $\approx$ 850 MeV obtained from the physical η' mass and chiral perturbation theory. Although we see approximate scaling, it would require calculations at larger values of β to rule out a significant lattice spacing effect. It is also worth remembering that the whole framework in which the quenched hairpin diagram is interpreted as a mass insertion is only demonstrably valid in the limit of large N_c, so some discrepency between the lattice calculation of m_0 and the phenomenological estimate might be expected. A recent calculation of the η' mass in two-flavor *full* QCD by the CPPACS collaboration [13] gave the result $m_{\eta'} = 960(87)^{+36}_{-286}$MeV, in good agreement with experiment. Detailed comparisons between quenched and full QCD studies of the η' should provide a better understanding of the accuracy of large-N_c arguments in the framework of chiral Lagrangians.

The overall size of quenched chiral loop effects is determined by the parameter δ, which can be computed from the hairpin insertion mass m_0 and the axial vector decay constant

f_A (evaluated in the next Section),

$$\delta = \frac{m_0^2}{24\pi^2 f_A^2}. \tag{21}$$

Using the chirally extrapolated values of m_0 and f_A, we obtain

$$\delta = .099(3), \quad \beta = 5.7 \tag{22}$$

and

$$\delta = .108(4), \quad \beta = 5.9. \tag{23}$$

It is interesting to consider not only the value of δ in the chiral limit, but also the effective value of δ at a given quark mass by computing the quantity (21) from the values of m_0 and f_A at that mass. The values of δ_{eff} vs. pion mass^2 for both $\beta = 5.7$ and 5.9 are plotted in Fig. 2. This plot shows a rather strong quark mass dependence of the effective QCL parameter, which may provide at least a partial explanation of the fact that many of the determinations of δ from lattice studies of quenched chiral logs [7] have favored a value of δ substantially smaller than the phenomenological estimate of $\delta \approx 0.17$. From Fig. 2 we see that, for pion masses > 300 MeV where most studies have been carried out, the value of δ_{eff} is smaller than the value in the chiral limit by as much as a factor two. The decrease of δ_{eff} with increasing quark mass represents the combined effect of a decreasing value of m_0 and an increasing value of f_A as the quark mass increases. Although the negative slope of δ_{eff} has the effect of suppressing quenched chiral logs, it is nevertheless more consistent to treat δ as a constant in fitting to chiral Lagrangian parameters, since the effective mass dependence should arise from higher order terms in the chiral expansion. This is the procedure we adopt in the subsequent analysis of the scalar and pseudoscalar correlators, where the best $Q\chi PT$ fit favors a value of δ about half as large as that obtained from the chirally extrapolated hairpin result. We might expect to find a larger value of δ

if studies were carried out well below $m_\pi = 300$ MeV. [It is interesting that a recent study [15] using overlap fermions, which went as low as $m_\pi = 180$ MeV, found a large value of δ. However, the value $\delta = 0.26(3)$ obtained in Ref. [15] is much larger than even our chirally extrapolated result of 0.108(4), indicating that there are other systematic differences in the calculations. Further chiral studies comparing different fermion actions on the same gauge configurations would be of considerable interest.]

The "allsource" quark propagators used to calculate the hairpin correlators [16] can also be used to calculate the topological susceptibility. Using the integrated anomaly method [17, 4], we calculate a winding number for each gauge configuration from the pseudoscalar charge integrated over the whole lattice. From these winding numbers, we compute the topological susceptibility $\chi_t = \langle \nu^2 \rangle / V$. Using the rho scale, this gives

$$\chi_t = (178(4)\ \text{MeV})^4, \quad \beta = 5.7 \tag{24}$$

$$= (171(3)\ \text{MeV})^4, \quad \beta = 5.9. \tag{25}$$

Results quoted previously [4] used the charmonium scale, which gives

$$\chi_t = (188(4)\ \text{MeV})^4, \quad \beta = 5.7 \tag{26}$$

$$= (190(3)\ \text{MeV})^4, \quad \beta = 5.9. \tag{27}$$

5 Pseudoscalar Masses and Decay Constants

The one-loop chiral Lagrangian analysis of the pseudoscalar and axial-vector propagators for the $\beta = 5.7$ ensemble has been described previously [4]. Here we briefly review that analysis and compare the previously reported results with the new results at $\beta = 5.9$. We also compare with results of the Alpha collaboration [7, 8] and discuss some issues associated with extracting the Leutwyler parameters L_5 and L_8, or correspondingly α_5 and

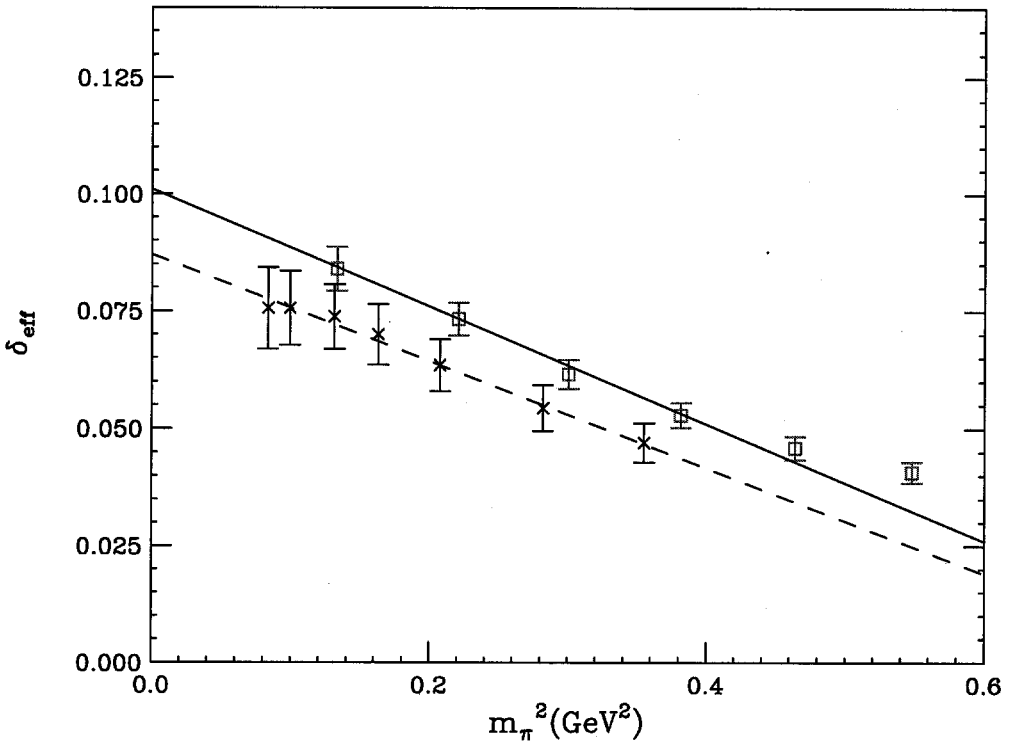

Figure 2: The quenched chiral log parameter δ_{eff} vs. squared pion mass. Results from both $\beta = 5.7$ ($\times$'s) and 5.9 (boxes) are plotted. The linear fits include all mass values for $\beta = 5.7$ and the four lightest masses for $\beta = 5.9$.

α_8. (Note: Here and elsewhere, we use a conventional notation for the rescaled parameters: $\alpha_i = 8(4\pi)^2 L_i$).

For both ensembles, we calculated propagators using smeared pseudoscalar, local pseudoscalar, and local axial-vector sources and sinks. The calculations were done for all meson propagators with both degenerate and nondegenerate quark masses. The chiral Lagrangian parameters were extracted from a global fit to all pseudoscalar masses and decay constants based on one-loop quenched χPT for the Lagrangian $\mathcal{L}_2 + \mathcal{L}_4 + \mathcal{L}_{hp}$, as discussed in Section 3. For the lightest pion masses we studied, finite volume effects on chiral loop integrals are potentially significant, so all one-loop calculations were carried out with the appropriate finite-volume momentum sums rather than loop integrals. In addition, quadratic and logarithmically divergent integrals are regularized by subtraction at a cutoff scale $\Lambda \approx \frac{1}{a}$. To summarize, a generic loop integral of the form

$$I_{ij} = \frac{1}{\pi^2} \int d^4p \frac{1}{p^2 + M_i^2} \frac{1}{p^2 + M_j^2} \tag{28}$$

is replaced by a cutoff momentum sum

$$I_{ij} = 16\pi^2 \sum_p \Big(D(p_i, M_i) D(p_j, M_j) - D(p, \Lambda)^2 \Big) \tag{29}$$

while a quadratically divergent integral

$$I_i = \frac{1}{\pi^2} \int \frac{d^4p}{p^2 + M_i^2} \tag{30}$$

is replaced by

$$I_i = 16\pi^2 \sum_p \Big(D(p, M_i) - D(p, \Lambda) - (\Lambda^2 - M_i^2) D(p, \Lambda)^2 \Big) \tag{31}$$

In these expressions, $D(p, M)$ is the free boson propagator and the momentum sums are defined according to the physical size of the corresponding lattice volume. With these

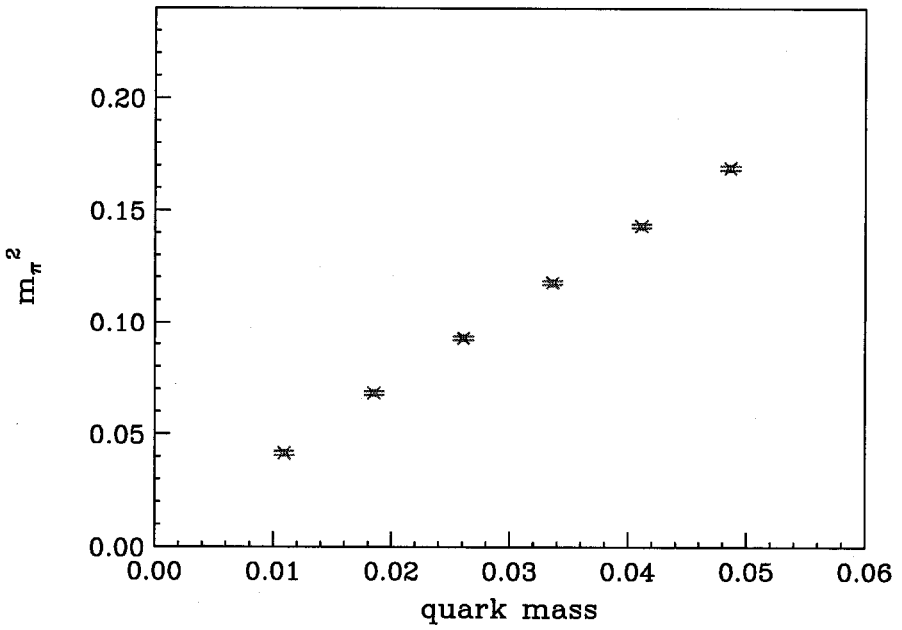

Figure 3: Pion mass squared m_π^2 for equal quark masses for the the $\beta = 5.9$ ensemble.

definitions, the value of the squared pseudoscalar meson mass up to first order in L_5, L_8, and δ is

$$M_{ij}^2 = \chi_{ij}(1+\delta I_{ij})\{1+\frac{1}{f^2}8(2L_8-L_5)\chi_{ij}[1 + \delta(\tilde{I}_{ij}+I_{ij})] + \frac{1}{f^2}8L_5\chi_{ij}\delta\tilde{J}_{ij}\} \quad (32)$$

where r_0 is a slope parameter, $\chi_i = 2r_0 m_i$, $\chi_{ij} = (\chi_i + \chi_j)/2$ and $m_i \equiv \ln(1+1/(2\kappa_i) - 1/(2\kappa_c))$. Here $\tilde{I}_{ij} = (I_{ii}\chi_i + I_{jj}\chi_j)/\chi_{ij}$,

$$J_{ij} \equiv \left(I_i + I_j - (M_{ii}^2 + M_{jj}^2)I_{ij}\right)/2, \quad (33)$$

$\tilde{J}_{ij} = J_{ij}/\chi_{ij}$. The loop integrals I_{ij} are defined in [4]. The fits for the pseudoscalar masses are shown in Figures 3-4.

For the pseudoscalar decay constants:

$$f_{P;ij} = \sqrt{2}fr_0(1+0.25\delta(I_{ii}+I_{jj}+2I_{ij}))\{1$$

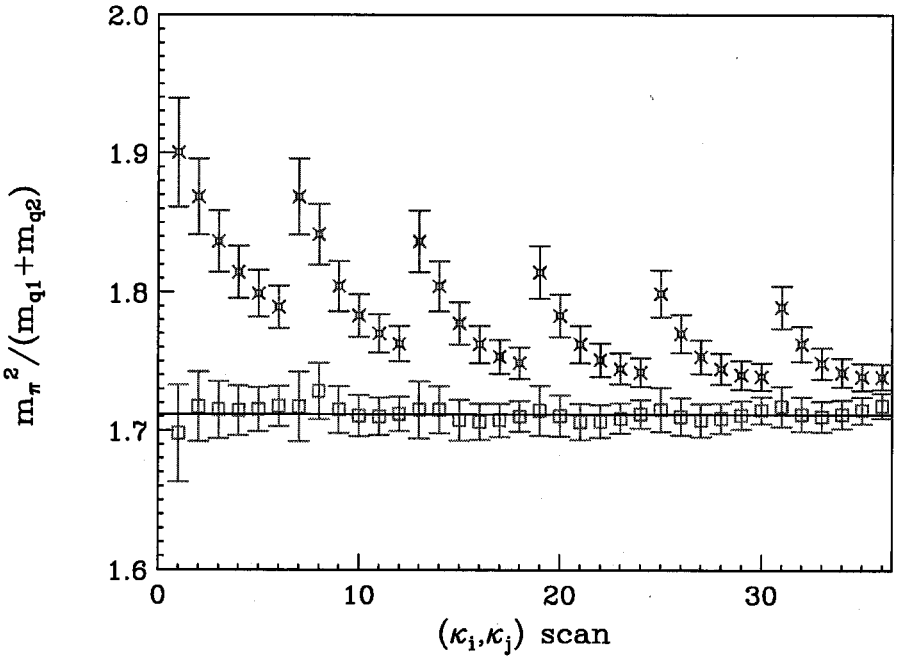

Figure 4: Chiral slope parameter scan for $\beta = 5.9$. Individual chiral slopes are denoted by $(\times)$. The scan number is $6 * (i-1) + j$ for the pair of κ values (κ_i, κ_j). The six κ values are ordered from lightest to heaviest quark mass. Also shown are the ratios to the chiral log fit (boxes) which yields a global average of 1.712(39).

$$+ \frac{4}{f^2}(4L_8 - L_5)\chi_{ij}[1 + \delta(\tilde{I}_{ij} + I_{ij})]$$
$$- \frac{4}{f^2}L_5\delta\chi_{ij}[(\frac{\tilde{I}_{ij}}{2} + I_{ij}) - (\tilde{J}_{ii} + \tilde{J}_{jj})]\} \quad (34)$$

The fits for the pseudoscalar decay constants are shown in Figures 5-6.

For the axial vector decay constants, we have:

$$f_{A;ij} = \sqrt{2}f(1 + 0.25\delta(I_{ii} + I_{jj} - 2I_{ij}))$$
$$\{\ 1 + \frac{4}{f^2}\chi_{ij}L_5[1 + \delta(2I_{ij} - \tilde{I}_{ij})]\} \quad (35)$$

The fits for the axialvector decay constants are shown in Figures 7-8. In Figures 4, 6, and 8 we show both the measured values and the ratio values where the fitted chiral log factors in Eqs. 32, 34 and 35 have been divided out. The results are scanned over all combinations of the quark mass values.

The chiral Lagrangian parameters listed in Table 3 are the result of a global correlated fit of the χPT expressions to masses and decay constants with both equal and unequal quark masses. The results obtained from this global fit are generally consistent with evaluations extracted from more limited fits to equal quark mass data. In particular, the value of L_5 may be estimated directly from the axial vector decay constant f_A. For equal quark masses f_A has no quenched chiral logs, so the mass dependence should be linear in the chiral limit,

$$f_A = A + Bm_\pi^2 \quad (36)$$

(Note that, in our notation, f_A includes a factor $\sqrt{2}$ relative to f_π, i.e. it's physical value is 132 MeV.) A determination of L_5 is obtained from the product of slope and intercept:

$$L_5 = \frac{A \cdot B}{8} \quad (37)$$

Note that A has units of *mass* and B has units of $(mass)^{-1}$, so that L_5 is dimensionless and can be evaluated without reference to a mass scale. We obtain the results (in GeV

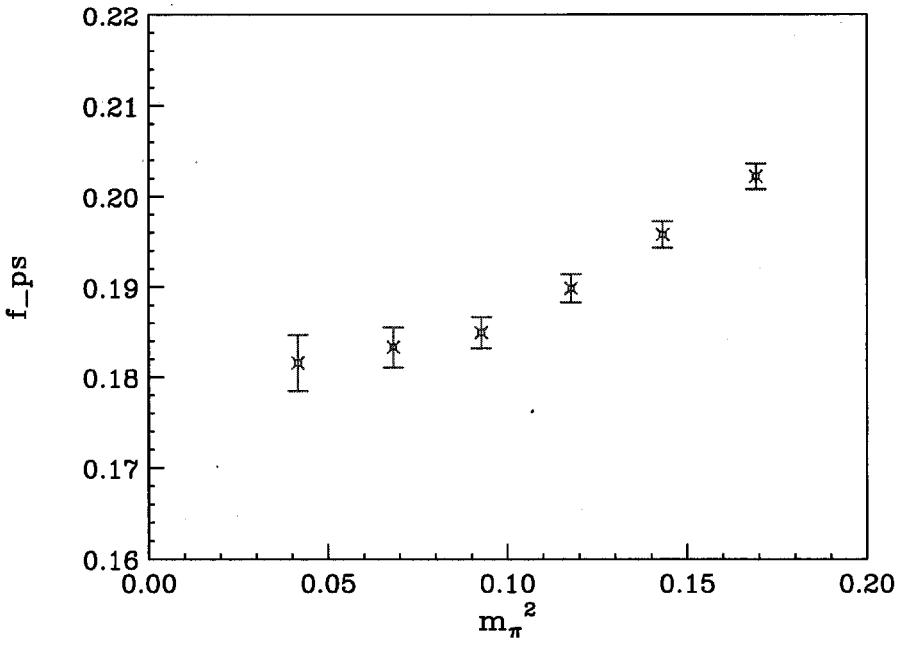

Figure 5: Pseudoscalar decay constant, $f_{\rm ps}$, versus pion mass squared, m_π^2 for the $\beta = 5.9$ ensemble. Only values for equal quark masses are shown.

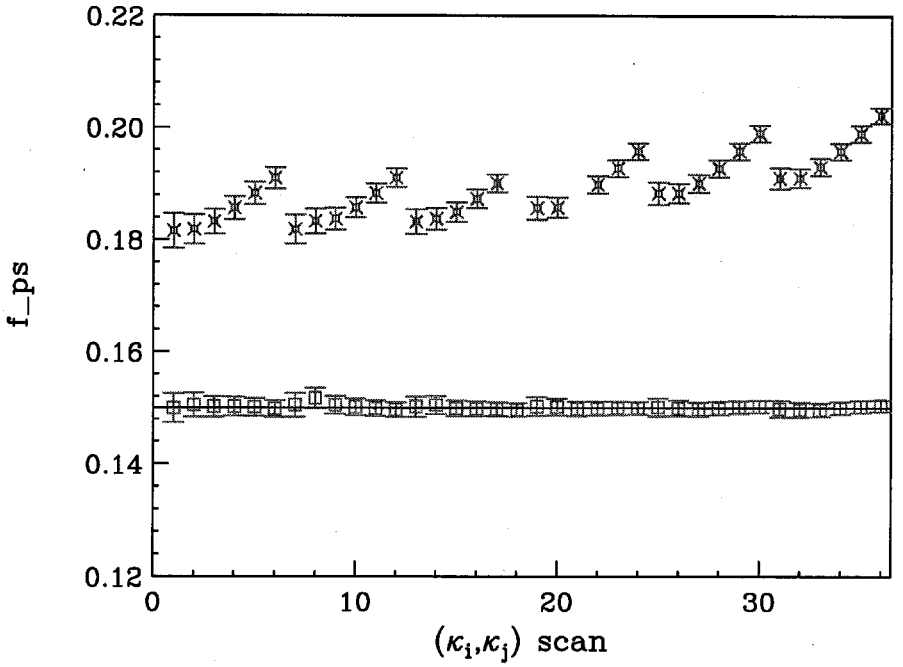

Figure 6: Pseudoscalar decay constant scan for $\beta = 5.9$. Also shown are the ratios to the chiral log fit which yields a global average $f_{\rm ps} = 0.1501(77)$. The (κ_i, κ_j) values are ordered as in Fig.4.

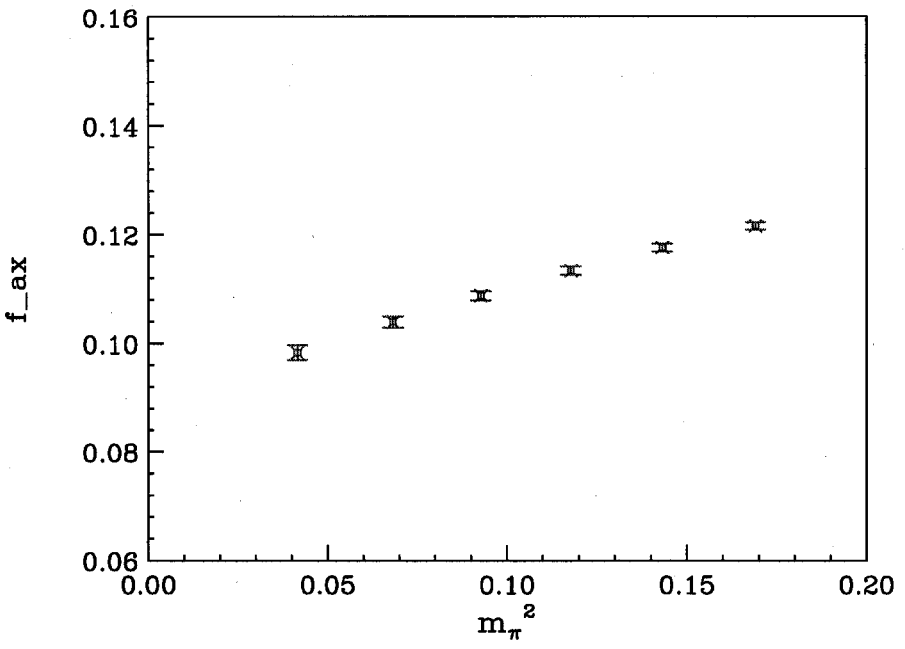

Figure 7: Axial vector decay constant, $f_{\rm ax}$, versus pion mass squared, m_π^2 for the $\beta = 5.9$ ensemble. Only values for equal quark masses are shown.

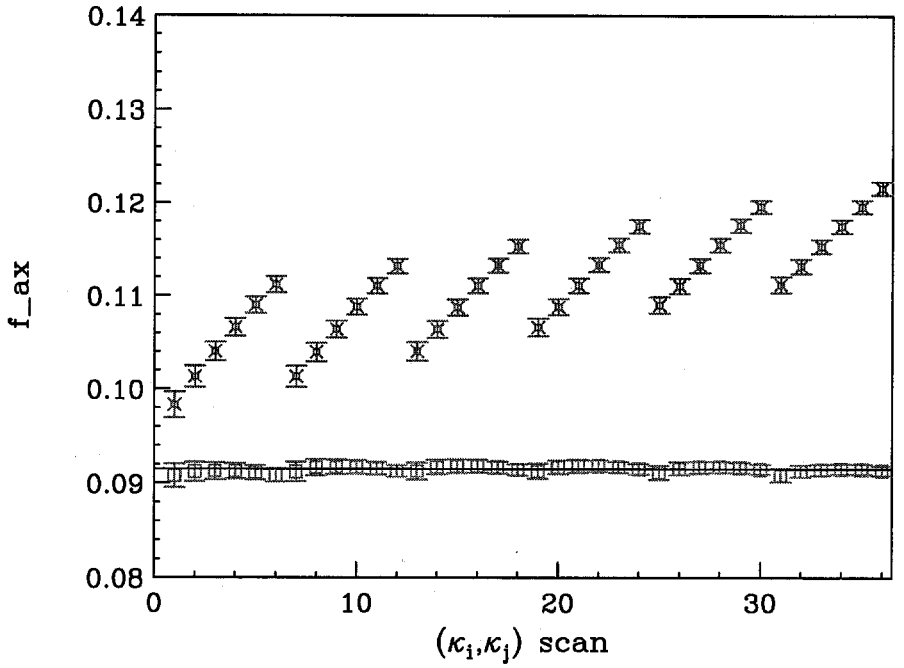

Figure 8: Axial vector decay constant scan, $f_{\rm ax}$ for $\beta = 5.9$. Also shown are the ratios to the chiral log fit which yields a global average $f_{\rm ax} = 0.0915(13)$. The (κ_i, κ_j) values are ordered as in Fig.4.

using the rho scale)

$$f_A = (.1653(17) + .117(5)m_\pi^2) \times Z_A \ \text{GeV}, \quad \beta = 5.7, \tag{38}$$

and

$$f_A = (.1515(20) + .106(7)m_\pi^2) \times Z_A \ \text{GeV}, \quad \beta = 5.9. \tag{39}$$

These fits are shown in Figs. 4, 6 and 8. Using $Z_A = 0.845$ and 0.865 for $\beta = 5.7$ and 5.9, respectively, we find

$$L_5(10^3) = 1.72(11), \quad \alpha_5 = 2.18(14), \quad \beta = 5.7 \tag{40}$$

and

$$L_5(10^3) = 1.50(9), \quad \alpha_5 = 1.89(11), \quad \beta = 5.9 \tag{41}$$

These values are consistent with the global fit results in Table 3.

A recent analysis of quenched data from the Alpha collaboration[8] obtained a value of $\alpha_5 = 0.99(6)$. Their analysis of the f_A ratios, $R_F(x)$, neglects a factor of

$$\frac{1}{(1 + y_{\text{ref}} \frac{1}{2}\alpha_5)} \tag{42}$$

(c.f Eq. (3.7)-(3.9) of [8]) reflecting the difference between χPT expansion about zero mass and their use of a large reference mass. Including this factor increases their estimate of α_5 to

$$\alpha_5 = 1.18(7). \tag{43}$$

If only statistical errors are considered, this estimate is still significantly below our values.

We can identify a number of differences in the two analyses which could account for much of the discrepancy. First, our data uses somewhat coarser lattices and an independent determination of the clover coefficient. This could affect the comparison with the Alpha analysis although they see little lattice spacing dependence in their data. There are also

Table 3: Best fit for the chiral Lagrangian parameters for the $\beta = 5.7$ and $\beta = 5.9$ lattices.

Parameter	$\beta = 5.9$	$\beta = 5.7$
$f = f_\pi$	0.091(2)	0.100(2)
$L_5 \times 10^3$	1.55(27)	1.78(35)
$(L_8 - L_5/2) \times 10^3$	0.02(5)	0.14(7)
r_0	1.71(8)	1.99(12)
δ	0.053(13)	0.059(15)

differences in methodology. Our results are obtained from a linear fit to $f_A(m_\pi^2)$ where the value of L_5 is determined from the dimensionless product of the slope and the intercept of the fit. This method is insensitive to physical scale parameter but is quite sensitive to the value of the axial-vector renormalization constant, being proportional to Z_A^2. In the context of the tadpole renormalization scheme [18] our results in Eqs. 40-41 include the perturbative renormalization constants $Z_A = 0.845$ and $Z_A = 0.865$ at $\beta = 5.7$ and $\beta = 5.9$, respectively. These values are derived from the perturbative formulas given in Ref. [19].

As an alternative method, we could determine the renormalization factors by requiring a fit to the physical value of $f_\pi = 93$ MeV. The result will now be sensitive to the choice of scale parameter. Fixing the scale with the rho mass, the renormalization constants are given by $Z_A = 0.80$ for $\beta = 5.7$ and $Z_A = 0.87$ for $\beta = 5.9$. Using these renormalization constants modifies our predictions to

$$L_5(10^3) = 1.54(10) \quad , \quad \alpha_5 = 1.95(13), \quad \beta = 5.7 \tag{44}$$

$$L_5(10^3) = 1.52(9) \quad , \quad \alpha_5 = 1.91(11), \quad \beta = 5.9 \tag{45}$$

This result is still substantially above the value obtained in the Alpha analysis. We note

that, in our results, the mass dependence of the tadpole renormalization factor contributes about 17% to the slope of $f_A(m_\pi^2)$. For linear extrapolations of $f_A(m_\pi^2)$ the above method is actually exactly equivalent to the Alpha ratio method with the inclusion of the correction factor (Eq. 42).

In the Alpha procedure, the physical value of f_π is used along with a particular choice of scale parameter. (This procedure, which involves the physical value of f_π, and/or m_ρ, is somewhat adhoc since the quenched values for f_π and m_ρ need not agree precisely with the Particle Data Group.) We note that caution is required in any direct comparison between the quenched and unquenched values of α_5. We have emphasized that there are no quenched chiral logs which affect the extrapolation of $f_A(m_\pi^2)$ for equal quark masses. However there is a strong chiral log effect in the unquenched theory. The Gasser and Leutwyler analysis[14] of the one-loop chiral logs determines α_5 from the physical values of f_K/f_π

$$\alpha_5 = 2.8 \pm 0.6 - 3\ln(\mu/m_\eta). \tag{46}$$

Hence, $\alpha_5 = 0.5$ for a large scale, $\mu = 4\pi f_\pi$, $\alpha_5 = .99$ for $\mu = 1$ GeV and $\alpha_5 = 1.76$ for $\mu = m_\rho$. The quenched theory really corresponds to the leading order of the $1/N_c$ expansion of the full theory which can not be isolated phenomenologically from the higher order contributions.

6 The Quenched Scalar Propagator

One of the most dramatic effects of quenched chiral loops is observed in the scalar valence propagator. The behavior of this propagator for the $\beta = 5.7$ ensemble was studied in [5]. There it was found that the propagator was well-described as a combination of a short-range positive exponential associated with a heavy (> 1 GeV) scalar $\bar{q}q$ meson state and a long-range *negative* tail arising from the η'-π intermediate state. In the quenched approximation,

the η'-π loop diagram exhibits not just a quenched chiral logarithm, but a quenched chiral *power*, with infrared behavior $\sim d^4p/p^6$. This long-range component is well-described in both shape and magnitude by the finite-volume η'-π loop calculation. [Note: In the $\beta = 5.7$ results, the ≈ 2 standard deviation discrepency between the data and the χPT calculation for $t > 7$ (c.f. Fig. 10 of Ref. [5]) we now believe to be a statistical fluctuation. See below.] As discussed in [5] the one-loop term that dominates the scalar propagator at small quark mass is determined with no adjustable parameters by the chiral Lagrangian parameters m_π, f, and r_0, already fixed from the analysis of the pseudoscalar sector. In particular, the long-range scalar propagator exhibits a very strong mass dependence in the light quark regime, which is very well explained by the dependence of the finite volume one loop contribution on m_π^2.

The analysis of the scalar correlator for $\beta = 5.9$ confirms the main conclusions of Ref. [5]. (See Figures 9-10) For the 5.9 ensemble, we find excellent agreement between the long-range behavior of the correlator and the $Q\chi PT$ loop calculation (which contains no adjustable parameters), with the theoretical formula matching the data all the way out to the largest time separation of $t = 16$. The details of the analysis of the $\beta = 5.7$ data were discussed in [5]. The $\beta = 5.9$ ensemble was analyzed similarly, though with some simplifications. First, in [5] both smeared and local sources were used, and a factorization procedure allowed an estimate of the mass of the excited a_0^* meson. This produced a good fit to the scalar correlator all the way down to t=1. For the analysis of the 5.9 data, we have not carried out an independent estimate of the excited a_0^* contribution, but have simply rescaled the parameters obtained from the 5.7 analysis, holding this contribution fixed in the fits which determine the ground state a_0 parameters. For the 5.9 data we used a time range $t \geq 3$, so the fits were insensitive to the choice of excited state parameters. The other difference in the 5.9 analysis is that the lightest pion mass (330 MeV) is somewhat heavier than that

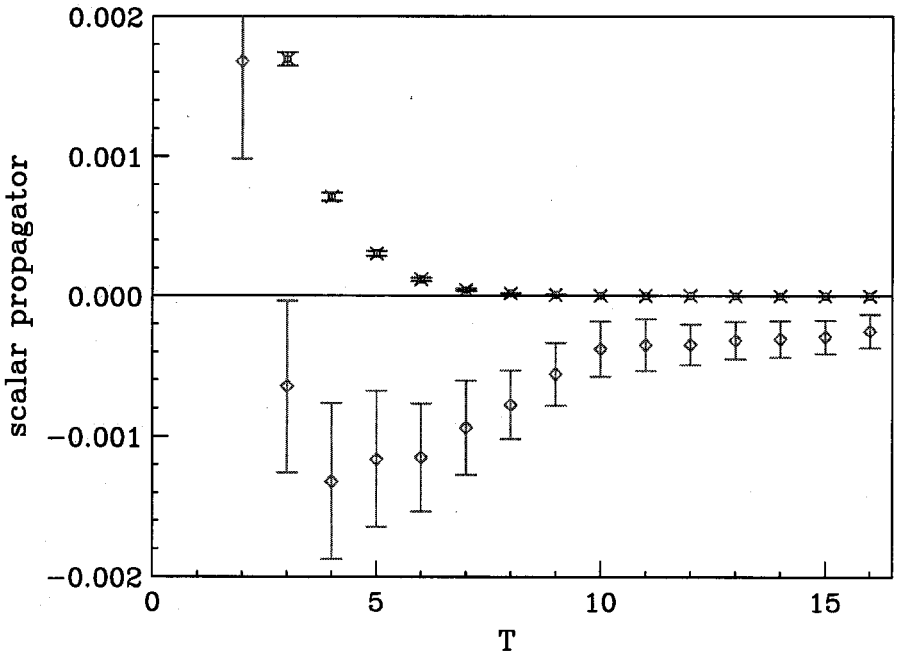

Figure 9: Isovector scalar correlator for the $\beta = 5.9$ $16^3 \times 32$ lattices. The lightest ($\kappa_q = \kappa_{\bar{q}} = .1397$) (red $\diamond$) and heaviest ($\kappa_q = \kappa_{\bar{q}} = .1382$) (blue x) correlators are shown.

for the 5.7 study (275 MeV). In [5] the formula used to parametrize the η'-π contribution was obtained by resumming iterated bubble graphs to all orders. In the analysis of the 5.9 data, we have found that only the one-loop graph is significant, so we have discarded higher order bubbles in the formula used to fit the correlator. Thus, defining the time-dependent zero-momentum scalar correlator as

$$\Delta(t) \equiv \sum_{\vec{x}} \langle \bar{\psi}_1 \psi_2(\vec{x}, t) \bar{\psi}_2 \psi_1(0) \rangle \tag{47}$$

we fit the lattice correlator to the function (c.f. Eq. (14) of Ref. [5])

$$\Delta(t) \sim 32 r_0^2 \frac{f_s^2}{2m_s} e^{-m_s t} + 4 r_0^2 \tilde{B}_{hp}(t) \tag{48}$$

where $\tilde{B}(t)$ is the $\vec{p} = 0$ Fourier transform of the η'-π bubble graph, calculated in a finite volume:

$$B_{hp}(p) = \frac{1}{VT} \sum_k \frac{1}{[(k+p)^2 + m_\pi^2]} \frac{-m_0^2}{(k^2 + m_\pi^2)^2} \tag{49}$$

Note that m_π, r_0, and m_0 are already determined from the pseudoscalar correlator analysis, so the only two fit parameters are the scalar mass and decay constant m_s and f_s. In Fig. 10 we show the data for the scalar correlator at $\beta = 5.9$ and the lightest quark mass, $\kappa = .1397$, along with a fit given by the function (48).

The mass of the a_0 meson obtained from our fits is plotted in Fig. 11. In the chiral limit we obtain (using the rho scale)

$$m_{a_0} = 1285(60)\ MeV \ \text{ at } \beta = 5.7 \tag{50}$$

$$= 1326(86)\ MeV \ \text{ at } \beta = 5.9 \tag{51}$$

In the chiral loop calculation of the η'-π intermediate state contribution, we have included the effect of finite physical volume, replacing momentum integrals by discrete sums.

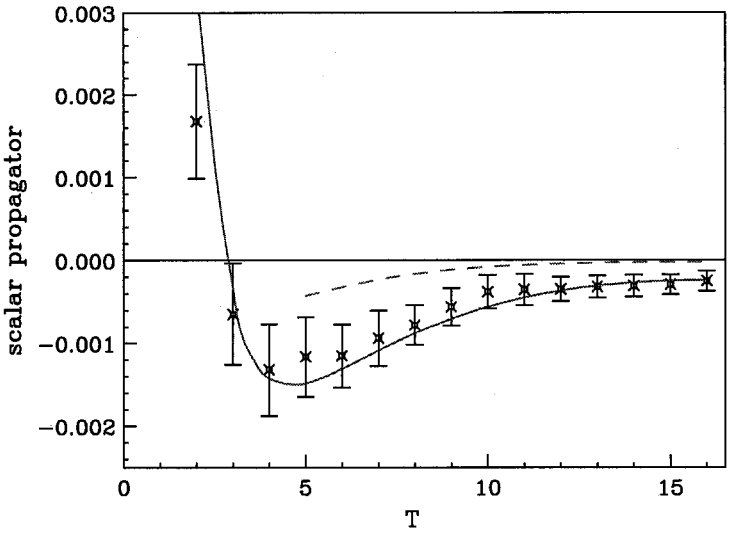

Figure 10: The scalar correlator for $\beta = 5.9$ and $\kappa = .1397$. The solid line is a fit consisting of the sum of a scalar meson pole and an η'-π loop diagram. The dashed line is the loop term in the infinite volume limit.

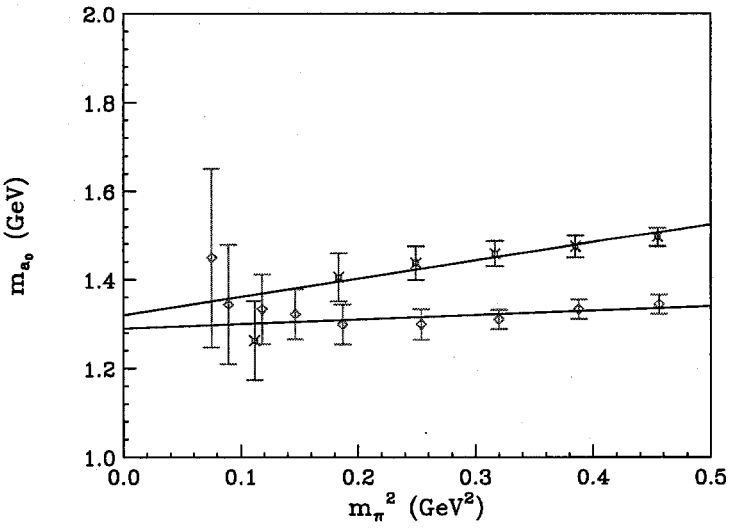

Figure 11: Mass of the a_0 meson for $\beta = 5.7$ (boxes) and $\beta = 5.9$ ($\times$'s).

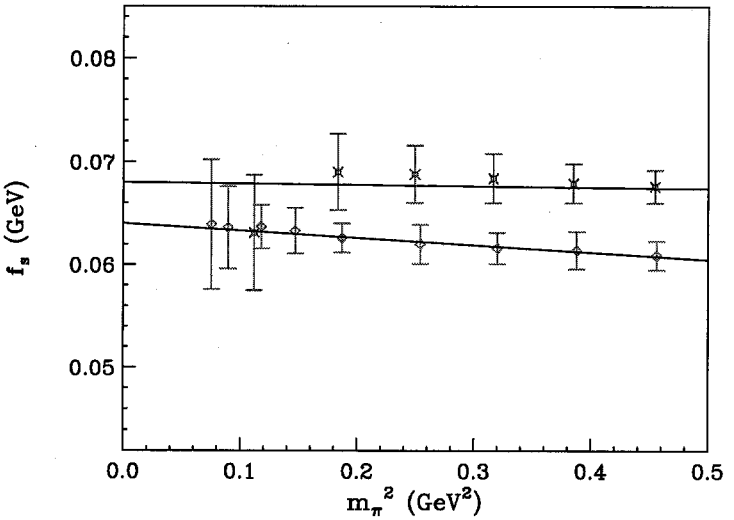

Figure 12: The scalar decay constant of the a_0 meson for $\beta = 5.7$ (boxes) and $\beta = 5.9$ ($\times$'s).

For the lightest pion masses the finite volume effect is quite large, due to the infrared behavior of the loop contribution. It is interesting to note that the Monte Carlo results for the scalar correlator agree quite nicely with the prediction of *finite volume* QχPT, but disagree significantly with the corresponding infinite volume calculation. This strong finite volume effect is also seen by the RBC collaboration[20]. The dashed line in Fig. 10 is the infinite volume loop calculation. For $t > 5$, the correlator is dominated by the η'-π loop, and it is clear that the Monte Carlo result exhibits the predicted enhancement from the finite volume effect. From the point of view of Dirac eigenmodes, the finite volume dependence predicted by χPT arises from a subtle interplay between exact zero modes and near zero modes. In the infinite volume limit, the contribution of exact zero modes vanishes, but for finite volume these modes are essential for reproducing the correct chiral behavior. Since the MQA pole shifting ansatz consists of repositioning some exact zero modes, it is reassuring to see that the resulting correlators exhibit excellent agreement with the finite volume

effect predicted by QχPT.

Finally, the scalar decay constant, f_s, of the a_0 meson obtained from our fits is plotted in Fig. 12. In the chiral limit we obtain (using the rho scale)

$$f_s = 64(5)\ MeV \ \text{ at } \beta = 5.7 \tag{52}$$

$$= 68(3)\ MeV \ \text{ at } \beta = 5.9 \tag{53}$$

7 Conclusions

The lattice calculations described in this paper and our previous works [4, 5, 6] have focused on the chiral properties of meson correlators in the flavor singlet and nonsinglet pseudoscalar and nonsinglet scalar channels. In addition to exhibiting for the first time a number of anomalous chiral effects due to quenching, the results have confirmed a level of overall consistency of the low energy chiral Lagrangian description of meson properties in QCD, and provided quantitative estimates of the relevant chiral Lagrangian parameters.

A central feature of this study is the accurate calculation of the pseudoscalar flavor-singlet hairpin insertion responsible for the gluonic component of the η' mass. In this calculation the MQA pole shifting ansatz has a particularly salutary effect. Since the pseudoscalar hairpin insertion arises from the $U_A(1)$ anomaly, it is particularly sensitive to topological features of the gauge field. As a result, the exceptional configuration problem in the hairpin is even more serious than in the valence correlators. The MQA procedure allows the first detailed study of the time-dependence of the hairpin correlator. The most striking feature of this time-dependence is that it is quite accurately described *at all time separations* by a the simple chiral Lagrangian diagram consisting of two pion propagators on either side of a momentum independent mass insertion. Values obtained for the field renormalization parameter α_Φ, which parametrizes the momentum dependence of the hairpin insertion,

are very small and consistent with zero. Perhaps even more remarkable is the fact that the hairpin correlator exhibits an absence of excited state contamination, with the ground-state double-pole diagram giving a complete description of the correlator. This result is confirmed not only by the time-dependence of the hairpin correlator, but also by a detailed comparison of hairpin and valence correlators with both smeared and local sources, as discussed in Ref. [4]. Since we know from the valence correlator that the local $\bar{\psi}\gamma^5\psi$ operator creates a state which includes a substantial excited state component along with the ground state pion, we conclude that these excited states are decoupled from the hairpin vertex itself. This may be viewed as a plausible extension of the OZI rule. Calculation of vector and axial-vector hairpin correlators [21] has confirmed that $q\bar{q}$ annihilation in these channels is highly suppressed compared to the anomaly-enhanced pseudoscalar hairpin diagram, as expected from OZI phenomenology. The absence of evidence for excited states in the pseudoscalar hairpin indicates that annihilation from these excited pseudoscalar states is similarly OZI suppressed. Only if the $q\bar{q}$ are in a Goldstone state do they have an unsuppressed pair-annihilation amplitude. The possibilities for extending these calculations to investigate the details of the connection between quark pair creation and annihilation and topological charge fluctuations are intriguing.

A global fit to the pseudoscalar masses and decay constants obtained from the valence (nonsinglet) correlators as a function of the quark masses yields an estimate of the quenched chiral log parameter δ, the pion decay constant f_π, the slope parameter r_0, and the Leutwyler parameters L_5 and L_8 (Table 3). We have found that a chiral Lagrangian analysis at the one-loop level provides a good description of the data over the range of masses studied, for both equal and unequal quark mass. The fit values of the quenched chiral log parameter δ, $\sim .05 - .06$, are rather small, but consistent with the values obtained directly from the hairpin diagram, averaged over the mass region studied. The chirally extrapolated value

of δ ($\sim$ .10) evaluated from the hairpin correlator is somewhat larger, but still smaller than the phenomenological estimate of $\sim$ 0.17. There may be some indication (cf. Fig. 2) that the value of δ is increasing for smaller lattice spacing so that, in the continuum limit, it might be closer to the phenomenological estimate. Similarly, the values of L_5 (α_5) we obtain are somewhat larger than the recent results of Heitger et.al. [8]. In any case, since the lattice spacings we have studied are fairly coarse, the overall consistency of our fits suggests that, even for finite lattice spacing, the low energy dynamics is well-described by a chiral Lagrangian, with the main lattice spacing effects consisting of corrections to the parameters.

The behavior of the nonsinglet scalar propagator at light quark mass provides a particularly useful probe of chiral dynamics, and the success of the chiral Lagrangian description (Section 6) is impressive. The prominent η'-π loop contribution is completely determined in terms of the chiral parameters m_π, r_0, and m_0, extracted from the pseudoscalar analysis. The loop calculation agrees well with the lattice data in magnitude, time-dependence, and pion mass dependence. For the box size ($\sim$ 2 fm) and pion masses we have used, the loop diagram exhibits a strong finite volume effect, and the agreement with the data is only satisfactory if the loop calculation is carried out in a finite volume. It would be interesting to carry out the numerical scalar propagator calculation on different size lattices to explicitly observe this finite volume effect. In view of the agreement we see on a single size box over a wide range of pion masses, we would expect the chiral loop diagram to also give a good description of the finite volume dependence, as long as the box is still large compared to the QCD scale. The sensitivity of the η'-π loop diagram to finite volume effects makes it especially useful for probing the role of zero modes in finite volume calculations. For extremely large boxes (large compared to the chiral scale), zero modes and global topology should be irrelevant, e.g. ensemble averages over any fixed topology should converge to the

same result in the infinite volume limit. On the other hand, for volumes which are large with respect to the QCD scale but still comparable to the chiral scale, the exact zero modes contribute in an essential way to the dynamics described by the chiral Lagrangian. The techniques developed here can easily be used to study the role of zero modes and global topology in finite volume chiral dynamics. This can be done, for example, by studying the contributions to the ensemble average for various correlators as a function of the global topological charge. We have seen that the integrated anomaly method of Smit and Vink [17], after MQA improvement, provides a convenient way of estimating the global topological index ν of a configuration. Calculation of ν using exactly chiral (e.g. overlap or domain wall) fermions would be ideal, but the approach used here based on clover improved Wilson fermions is more economical and appears to be quite effective for studying issues which do not depend crucially on having exact integer valued ν's. For example, the results for the topological susceptibility (Section 4) are in good agreement with other estimates. It would be interesting to carry out a more detailed investigation of the scalar and pseudoscalar correlators studied here, decomposing the ensemble averages into various topological charge sectors. This would provide useful insight into the role of global topology in chiral dynamics at finite volume.

After properly accounting for quenched chiral effects in the scalar propagator, the a_0 masses (at κ_c) are extracted. The results, $m_{a_0} = 1.33(5)$ and $1.34(6)$ GeV for $\beta = 5.9$ and 5.7 respectively are considerably larger than the observed $a_0(980)$ resonance mass. The value for $m_{a0} = 1.33(5)$ GeV suggests that there is a large effect when internal quark loops are included or that the observed $a_0(980)$ resonance is a distinct state, possibily a $K\bar{K}$ "molecule" (which would not appear in the quenched approximation), and not an ordinary $q\bar{q}$ meson.

Acknowledgements

The work of W. Bardeen and E. Eichten was performed at the Fermi National Accelerator Laboratory, which is operated by University Research Association, Inc., under contract DE-AC02-76CHO3000. The work of H. Thacker was supported in part by the Department of Energy under grant DE-FG02-97ER41027.

References

[1] S. R. Sharpe and N. Shoresh, Phys. Rev. D **62**, (2000) 094503.

[2] C. Bernard and M. Golterman, Phys. Rev. D **46** (1992) 853

[3] S. Sharpe, Phys. Rev. D46 (1992) 3146. Rev. D46 (1992) 853.

[4] W. Bardeen, A. Duncan, E. Eichten and H. Thacker, Phys. Rev. D **62**, 114505 (2000) [arXiv:hep-lat/0007010].

[5] W. Bardeen, A. Duncan, E. Eichten, N. Isgur and H. Thacker, Phys. Rev. D **65** (2002) 014509.

[6] W. Bardeen, E. Eichten and H. Thacker, "Low energy chiral Lagrangian parameters for scalar and pseudoscalar mesons," arXiv:hep-lat/0209164

[7] H. Wittig, "Chiral effective Lagrangian and quark masses," arXiv:hep-lat/0210025.

[8] J. Heitger, R. Sommer and H. Wittig [ALPHA Collaboration], Nucl. Phys. B **588**, 377 (2000)

[9] W. Bardeen, A. Duncan, E. Eichten, G. Hockney and H. Thacker, Phys. Rev. D57 (1998) 1633.

[10] R. Frezzotti, S. Sint and P. Weisz [ALPHA collaboration], JHEP **0107**, 048 (2001) [arXiv:hep-lat/0104014]; R. Frezzotti, P. A. Grassi, S. Sint and P. Weisz [Alpha collaboration], JHEP **0108**, 058 (2001) [arXiv:hep-lat/0101001].

[11] R. Narayanan and H. Neuberger, Phys. Rev. Lett. **71**, 3251 (1993) Nucl. Phys. B **443**, 305 (1995).

[12] D. B. Kaplan, Phys. Lett. B **288**, 342 (1992).

[13] V. I. Lesk *et al.* [CP-PACS Collaboration], arXiv:hep-lat/0211041.

[14] J. Gasser and H. Leutwyler, Nucl. Phys. B250 (1985) 465.

[15] T. Draper, S. J. Dong, I. Horvath, F. Lee, K. F. Liu, N. Mathur and J. b. Zhang, arXiv:hep-lat/0208045.

[16] Y. Kuramashi, M. Fukugita, H. Mino, M. Okawa and A. Ukawa, Phys. Rev. Lett. **72**, 3448 (1994).

[17] J. Smit and J. C. Vink, Nucl. Phys. B **286**, 485 (1987).

[18] G. P. Lepage and P. B. Mackenzie, Phys. Rev. D **48**, 2250 (1993) [arXiv:hep-lat/9209022].

[19] T. Bhattacharya and R. Gupta, Phys. Rev. D **54**, 1155 (1996) [arXiv:hep-lat/9510044]; A. X. El-Khadra, A. S. Kronfeld, P. B. Mackenzie, S. M. Ryan and J. N. Simone, Phys. Rev. D **58**, 014506 (1998) [arXiv:hep-ph/9711426].

[20] S. Prelovsek and K. Orginos [RBC Collaboration], "Quenched scalar meson correlator with domain wall fermions," arXiv:hep-lat/0209132.

[21] N. Isgur and H. B. Thacker, Phys. Rev. D **64**, 094507 (2001) [arXiv:hep-lat/0005006].